

## Supporting Information

### **Noble-Metal-Free Recyclable Electronic Nanoinks for Wireless Wearable Sensors**

*Naimul Arefin,<sup>1§</sup> Kwame Afrifa Obeng Ofori,<sup>2§</sup> Curtis Borden,<sup>2</sup> Nishat Paul,<sup>1</sup> Thomas Jones,<sup>1</sup> Nicolas Constantinides,<sup>1</sup> Kai Wu,<sup>2\*</sup> Minxiang Zeng<sup>1\*</sup>*

1. Department of Chemical Engineering, Texas Tech University, Lubbock, TX 79409, USA

2. Department of Electrical and Computer Engineering, Texas Tech University, Lubbock, TX 79409, USA

\*Email: [minzeng@ttu.edu](mailto:minzeng@ttu.edu) and [kai.wu@ttu.edu](mailto:kai.wu@ttu.edu)

§ Naimul Arefin and Kwame Afrifa Obeng Ofori contributed equally to this work.

## Supporting Information

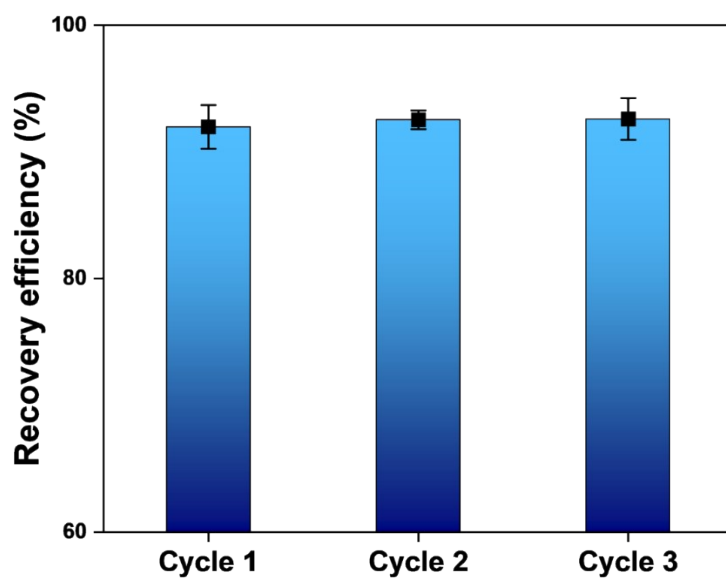


**Figure S1. Recovery efficiency of the printed conductors across three cycles of recycling.**

## Supporting Information

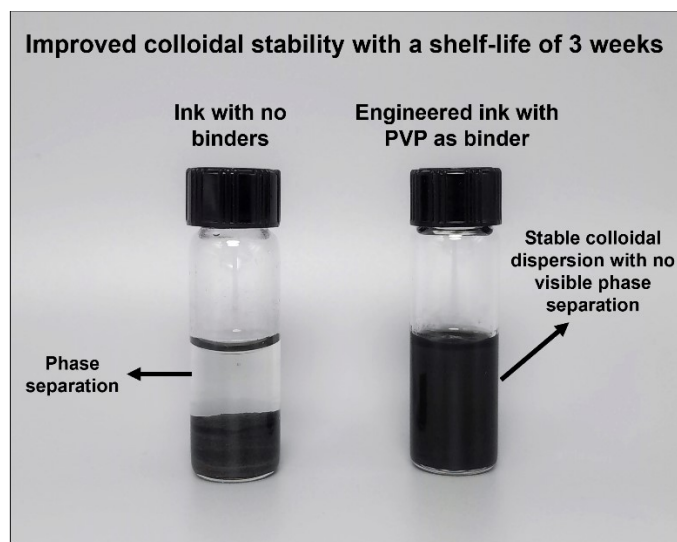


**Figure S2. Optical image of the formulated ink showing improved colloidal stability achieved through ink engineering (no visible sedimentation).**

## Supporting Information

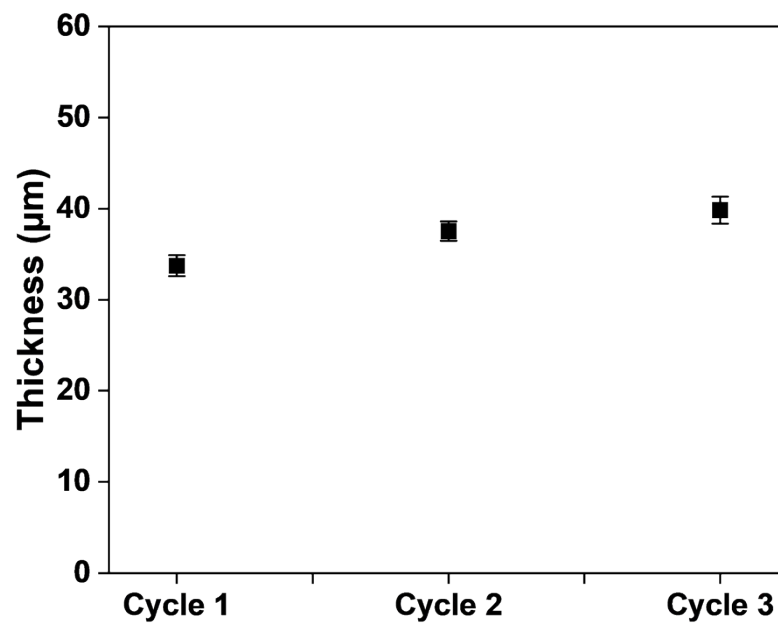


**Figure S3. Average line thickness of the printed sensors across three recycling cycles.**

## Supporting Information

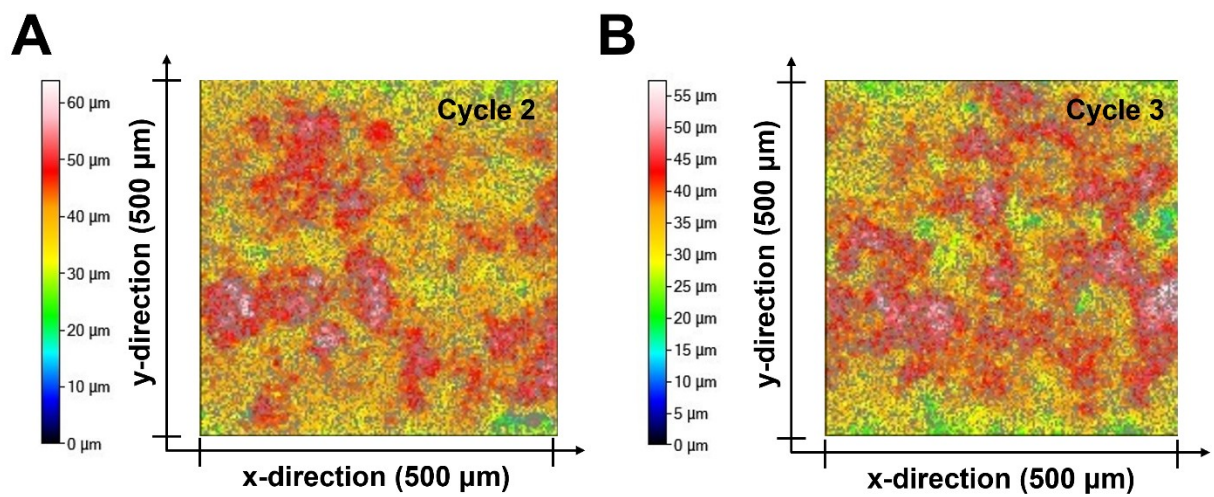


**Figure S4.** Surface topology of the printed sensor from A. recycling cycle 2; B. recycling cycle 3.

## Supporting Information

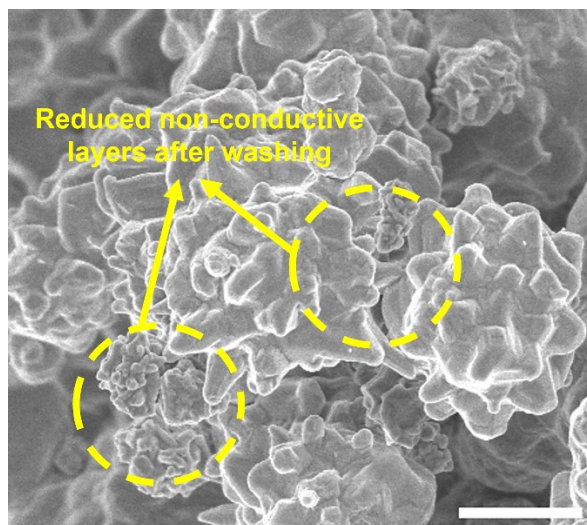
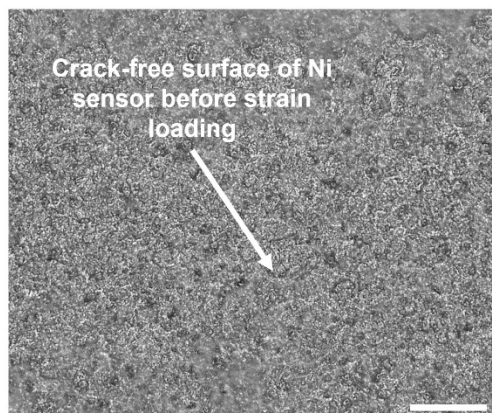


**Figure S5.** Surface morphology of the Ni particles after washing treatment with DMF, showing reduced non-conductive layers. (scale bar 1  $\mu\text{m}$ ).

**A**



**B**

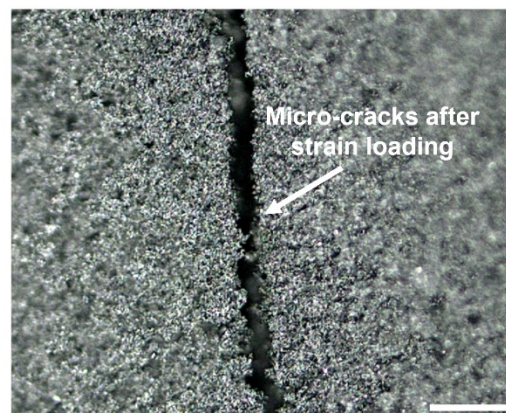


**Figure S6. Surface morphology of the printed Ni sensor; A. Before strain loading (scale bar 200  $\mu\text{m}$ ); B. After strain loading (scale bar 100  $\mu\text{m}$ ).**

## Supporting Information

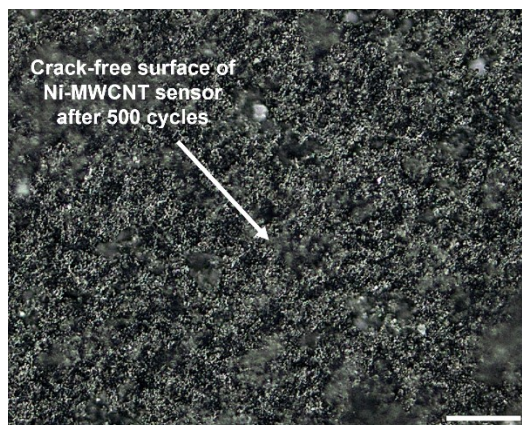


**Figure S7. Surface morphology of the printed Ni-MWCNT sensor after 500 cycles of strain loading at 0.8% strain (scale bar 100  $\mu\text{m}$ ).**

## Supporting Information

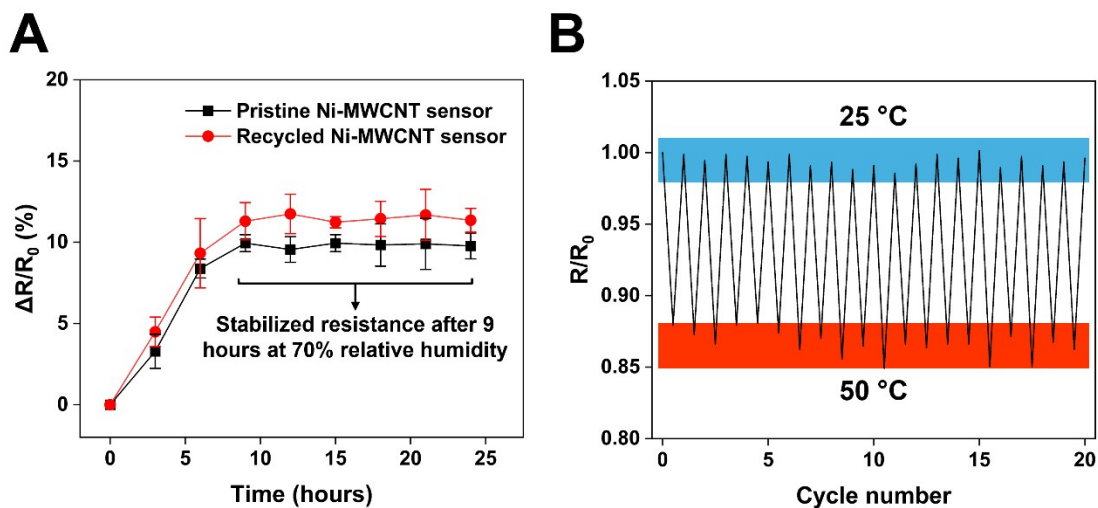


**Figure S8. Chemical and thermal stability of the Ni-MWCNT sensors; A. Change in relative resistance of the pristine and recycled sensors over a 24-hour time period under 70% relative humidity (RH); B. Normalized resistance of the Ni-MWCNT sensor under cyclic heating and cooling between 25 °C and 50 °C.**

## Supporting Information

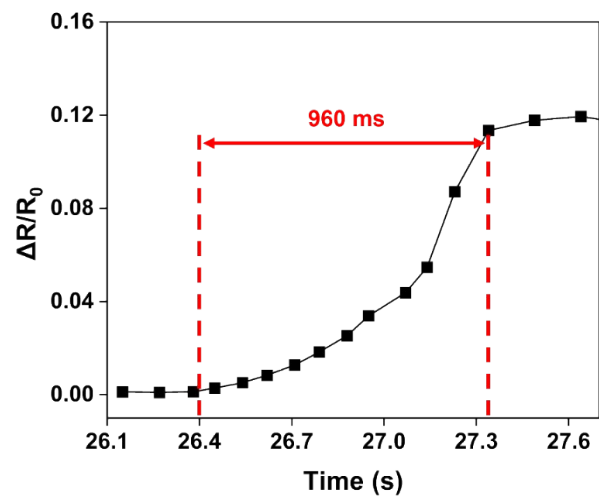


**Figure S9. Response time of the wireless sensing platform under 0.8% strain.**

## Supporting Information

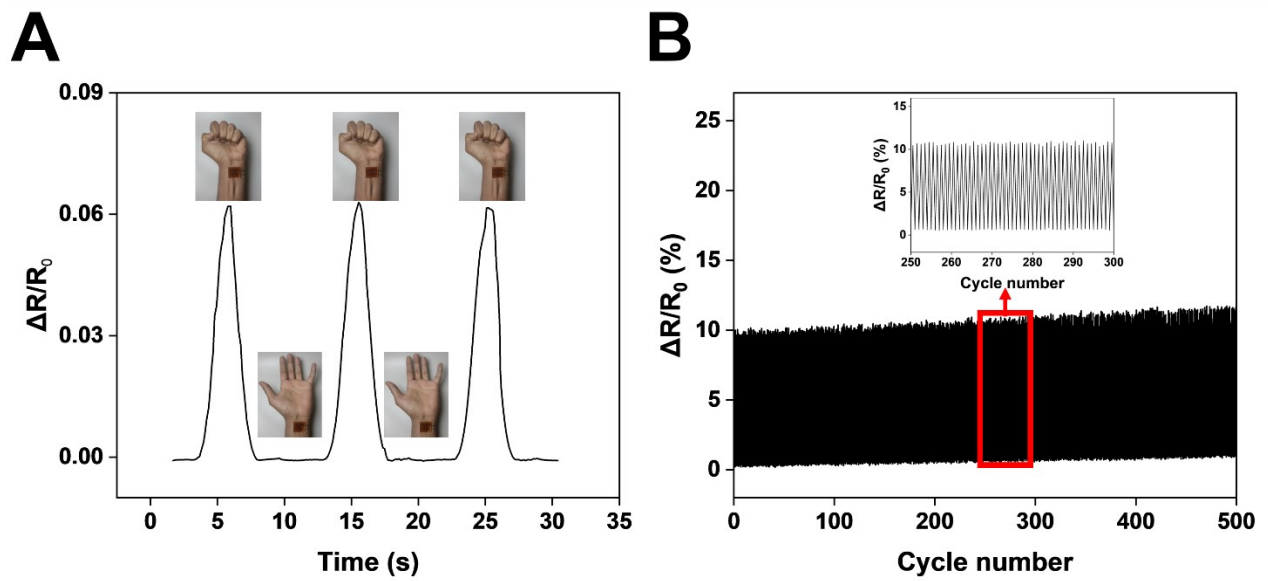


**Figure S10. Sensing performance and mechanical stability of the recycled Ni-MWCNT sensor; (A) Response signal of the Ni-MWCNT strain sensor during making a fist; (B) Change in relative resistance of the strain sensor during 500 cycles of stretching and releasing at 0.8% strain.**

## Supporting Information

**Table S1.** Dimensions of the printed sensors. The thickness was measured using an optical profilometer, and the line width was estimated using optical microscopy. The path length, bulk width, and bulk length are collected directly from the sensor design.

<b>Recycling cycle number</b>	<b>Line thickness (<math>\mu\text{m}</math>)</b>	<b>Line width (mm)</b>	<b>Path length (mm)</b>	<b>Bulk width (mm)</b>	<b>Bulk length (mm)</b>
1	33.73 $\pm$ 1.16	1.01 $\pm$ 0.025	180	12.5	20
2	37.52 $\pm$ 1.07	0.99 $\pm$ 0.017	180	12.5	20
3	39.81 $\pm$ 1.07	1.01 $\pm$ 0.02	180	12.5	20